Title
High lithium sulfide loading electrodes for practical Li/S cells with high specific energy

Authors
Sun, Dan
Hwa, Yoon
Zhang, Liang
et al.

Publication Date
2019-10-01

DOI
10.1016/j.nanoen.2019.103891

Peer reviewed

High lithium sulfide loading electrodes for practical Li/S cells with high specific energy

*Dan Sun, Yoon Hwa, Liang Zhang, Jingwei Xiang, Jinghua Guo, Yunhui Huang and Elton J. Cairns**

Dr. Dan Sun, Dr. Yoon Hwa, Prof. Elton J. Cairns
Energy Technologies Area, Lawrence Berkeley National Laboratory, Berkeley, CA 94720, United States

Prof. Elton J. Cairns
Department of Chemical and Biomolecular Engineering, University of California, Berkeley, CA 94720, United States
E-mail: ejcairns@lbl.gov

Dr. Liang Zhang, Prof. Jinghua Guo
Advanced Light Source, Lawrence Berkeley National Laboratory, Berkeley, California 94720, United States

Jingwei Xiang, Prof. Yunhui Huang
Department of Materia Science and Engineering, Huazhong University of Science and Technology, Wuhan, Hubei, 430074, China

Keywords: (lithium/sulfur cell, lithium sulfide, high loading, electrolyte/sulfur ratio, aluminum foam)

Abstract: To date, Li_2S has drawn significant attention as a positive electrode active material for LIBs due to its high theoretical specific capacity and capability of pairing with a lithium-free anode which can obviate the safety concerns of the lithium metal anode when using sulfur. In recent years, various approaches have been employed to successfully develop Li/Li_2S rechargeable cells toward commercial cells that meet the power source performance goals for high energy/power applications. It is expected that high lithium sulfide-loading cells with long cycle life, excellent capacity delivery and low E/S ratio can be achieved. Here, we report a Li_2S electrode consisting of a novel Li_2S/KB@Cf nano-composite which delivers high areal capacity (7.56 mAh cm^{-2}) and excellent cycling stability with high mass loading(11.29 mg cm^{-2}) and a robust 3-dimensional (3D) Al foam with high open area as

current collector. The high conductivity and scalability of active material, the availability of 3D conductive accommodation for electrode material and the control of electrolyte/sulfur ratio offer the potential of realization of practical applications using Li/S cells.

1. Introduction

The development of the Li-ion battery (LIB) has led to a portable electronics revolution during last couple of decades,[1] however, the traditional LIBs seem to be insufficient for practical applications in some emerging markets such as electronic vehicles (EVs) and aircraft that are powered by rechargeable batteries due to the limited specific energy of the cell. For mass market conversion to electric vehicles, rechargeable battery systems of high specific energy (> 300 Wh kg^{-1}) and low-cost are required.[2] Among all alternatives, the lithium/sulfur (Li/S) cell has been considered most promising due to its low cost, high abundance and environmentally benign sulfur, ultrahigh theoretical specific energy (2,680 Wh kg^{-1}) and theoretical energy density (2967 Wh L^{-1}) which far exceed those of conventional lithium-ion cells. Furthermore, good safety and especially, the technical similarity of cell manufacturing processes of the Li/S cell to that of Li ion cells are strong advantages for adoption of the Li/S cell by the battery industry. Notwithstanding, the large-scale pratical application of the Li/S cell has been impeded due to some inrinsic drawbacks such as low conductivity of both sulfur and its dicharge product (lithium sulfide), large volume change during discharge and charge processes and the dissolution of polysulfides into most organic solvents.[3]

Recently, pre-lithiated S, lithium sulfide (Li_2S) has been proposed to be a more desirable electrode material because it permits the cell to be assembled in the discharged state and avoid the mechanical degradation of the sulfur electrode associated with the volume expansion of sulfur (up to 78%) during discharge.[4] Many strategies have been applied in an attempt to promote the development of the Li/S system,[5] nevertheless, after extensive study of sulfur and lithium sulfide electrodes, neither of these technologies has been commercialized due to

poor long-term cycle life and low demonstrated specific energy of lithium/sulfur cells.[6] Practical applications require high sulfur loading electrodes together with the lowest posssible "dead weight" (the total weight of all cell components except that of the active electrode materials) such as electrolyte, electrode additives (polymeric binder and carbon) and cell housing, while maintaining good performance.[3e, 3f] This is quite challenging because all the drawbacks become more severe when the sulfur loading exceeds the practical acceptable level (>3 mg cm^2). Most commerical current collectors have limitations related to the loading, sulfur utilization and structural stability. Due to the insulating nature of S and Li_2S, the addition of a significant amount of conductive material into the high loading electrodes is required and introduces more surface area, and thus more electrolyte is needed.[7] A certain amount of binder is necessary to hold the electrode materials together and bond them to the current collector to maintain good conductivity and mechanic stability of the electrode.[8] Among all the cell components contributing to the "dead weight", the electrolyte is very influential because it is an essential component to support the electrochemical reactions by wetting the active materials properly and providing the necessary ionic path, which indicates that reducing the electrolyte amount needs to be done thoughtfully.[9]

The energy density calculations for pouch cells with an excess of 100% of lithium metal (**Figure S1**) yield the conclusion that a higher active material loading and S utilization together with lower electrolyte/S (E/S) ratio can lead to the expectation that the practical Li/S cell can meet the 350 Wh/kg goal for EV applications. Technically, in order to achieve Li/S cells with high specific energy, long cycle life and high safety, each parameter of the cell components should be optimized, as demonstrated in **Figure 1**.[3f, 7b] Here, in this paper, we report the development of a Li/Li_2S cell with a novel Li_2S/KB@Cf composite as active material and a robust 3-dimensional (3-D) Al foam current collector. A coin cell assembled with a Li_2S mass loading of 11.29 mg cm^{-2} can deliver an aerial capacity of 7.56 mAh cm^{-2} after 100 cycles with an electrolyte/sulfur (E/S) mass ratio of 5.5. Also, the 3x4 cm^2 2-

electrode pouch cell (Li_2S mass loading: 10.2 mg cm^{-2}, Li_2S content: 75 %wt.) with a E/S ratio as 4.4 was developed, which exhibited an areal specific capacity of 7.96 mAh cm^{-2}. The yields are relatively high and the synthesis process is facile and readily practical.

2. Results and Discussion

2.1. Active Material Preparation

Figure 2 schematically illustrates the fabrication process of Li_2S/KB@Cf nano-composite and Li_2S electrode. In order to have controlled fine particle size of Li_2S, commerial Li_2SO_4 was re-precitated to get a relatively uniform size around 2~5 um, as shown in **Firgure S2**. The Li_2S/KB@Cf composite was produced through a carbon-thermal reduction of Li_2SO_4 followed by the in-situ formation of a carbon protective layer and carbon nano fibers via a Chemial Vapor Deposition (RCVD) process.[10] The addition of PVP during the preparation provides a good dispersion of Ketjen Black(KB) in aqueous solution and strong adhesive strength between KB and Li_2SO_4 particles, which further results in more uniform and durable carbon protection of as-sythesized Li_2S/KB. X-ray diffraction (XRD) pattens and scanning electron microscopy (SEM) characterization help to identify the crystal structure and mophology of the Li2S/KB composite under the influence of PVP and the amount of KB. As shown in **Figure 3**(g), all XRD peaks observed in the XRD patterns of the prepared Li_2S/KB composites with different Li2S fractions can be indexed by the cubic structure of Li_2S (Fm3m, PDF#65-2981), indicating that pure Li_2S was successfully fabricated in all samples. SEM results displayed in Figure 3(a-f) indicate that PVP played an important role in adhering KB onto Li_2S particles which is beneficial for the reduction of resistance and suppressing the polysulfide dissolution into the electrolyte during the charge/discharge processes. The protection by the compact KB layer was also confirmed by XRD results tested in ambient air atomosphere shown in **Figure S3**; only LiOH peaks appeared in the Li_2S sample whreas the sample synthesized with PVP still maintained the Li_2S structure.

To get the first view of the electrochemical performance of different electrode compositions, coin cells with Li_2S loadings around 1.5 mg cm^{-2} were tested at different C rates. As shown in Figure 3(h), Li_2S/KB composites synthesized with PVP show improved cell capacities and rate capabilities, which is in agreement with the SEM results. Li_2S/carbon composites have been intensively incestigated for developing advanced Li_2S elecrodes since most carbonaceous materials have good electronic conductivity which can compensate for the inadequate electronic conductivity of both Li_2S and sulfur, resulting in improved rate capability and sulfur utilization.[6c, 11]

Here in this work, the carbon protection of the Li_2S/KB composite is composed of carbon derived from the carbonization of the remaining PVP and excess KB. Theoretically, carbonaceous material with a higher specific surface area can provide a higher specific capacity,[6a, 12] however, the high porosity and low density of KB lead to a lower mechanical stability of the electrode structure and a need for a larger amount of electrolyte. By controlling the synthesis process, the Li_2S/KB composite with 80 wt.% of Li_2S proved to exhibit the best performance. With further RCVD treatment, a conformal carbon deposition together with carbon nano fibers with diameters around 30nm were produced, which could be attributed to the trace amount of Fe(50 ppm by weight) contained in KB(EC600JD), as shown in **Figure 4**(a).

Further insight into the structure of the carbon fibers was provided by transmission electron microscopy(TEM) after washing away all the Li_2S, as shown in Figure 4(b), indicating the graphitic structure of the as-synthesized fibers. The amount of CNFs can be adjusted by controlling the time of the RCVD procedure, as shown in **Figure S4**. Considering the requirement for a high Li_2S fraction and high specific energy, the total carbon amount in the active material was controlled between 15-20 wt.%. Figure 4(c) shows the XAS spectrum of

the as-synthesized Li_2S/KB@Cf composite; the spectrum exhibits two main features at ~ 2473.2 and ~2475.7 eV, respectively, which agrees with previous reports.[6g, 13]

Due to the high conductivity of the KB particles and the continuous structure of the carbon fibers as synthesized which can provide very stable and effective electron conduction pathways, no more carbon additives are needrd in the electrode while preparing the slurry, resulting in a higher Li_2S fraction (>70 wt.%) and less "dead weight" in the cell.[14] The long-term cycling stability of the relatively lower S loading (3.72 mg cm^{-2} of Li_2S, 2.58 mg cm^{-2} of S) electrode with an aluminum foil current collector was conducted at a current density of 0.8 mA cm^{-2} and a E/S ratio of 20 for 200 cycles, the results are shown in Figure 4(d). A specific capacity of 596 mA·h g^{-1} of Li_2S (855 mA·h g^{-1} of S) was obtained after a cycling period of 200 cycles with a Coulombic efficiency of over 97%. However, due to the mechanical limitations of aluminum foil, a capacity retention of only 75.6% was achieved after 200 cycles. The large overpotential observed in Figure 4(e) also is consistent with low electronic conductivity of the electrode. By investigating the IR drop during discharge of an electrode with higher Li_2S loading the (**Figure S5**) using Al foil, ionic conductivity of the electrode was shown to be a problem which resulted in poor cycle life and low specific energy.

2.2. High Li_2S loading electrodes

Typically, the current collector works as an electronic connection between the active material and the external circuit. The curent collector must offer good surface conditions for obtaining strong adhesion to the active material as well as the proper geometry with stability and flexibility. Most recently, various conductive frameworks have been proposed as current collectors.[3e, 7b, 15] Here in this work, in order to obtain stable long-term cycling performance with higher S loadings than 3 mg cm^{-2}, a robust 3-dimensional (3-D) current collector, aluminum foam, was introduced. As shown in **Figure 5** (a, b), the aluminum foam consists of pores with different sizes varying from 100 um to 500 um which are beneficial to

accommodating the active material as well as electrolyte in its interior space. The continuous metallic structure also can help deliver electrons to the entire sulfur electrode. Enhanced both ionic and electronic conductivity makes the 3D current collector a decisive factor in high loading cells. Scanning electron microscopy (SEM) images (Figure 5c-f) reflect electrode strutures with different S loadings using aluminum foam as the current collector. Electrode material was uniformly distributed inside of the channels. Due to the special mechanical structure of Al foam, it's possible to increase the active material loading to as high as 15 mg cm^{-2}.

Due to the high elctronic conductivity of the prepared Li_2S/KB@Cf nanocomposite and the special structure of Al foam, an active material slurry with a high Li_2S fraction of 75% by weight could be prepared and the performance was elctrochemically evaluated. After further optimization of the electrolyte, 0.5M LiTFSI in DOL/DME (1:1, by volume) was uesd as electrolyte for its lower viscosity and relatively high ionic conductivity and stability. $LiNO_3$ was also employed as an electrolyte additive because it not only helps the electrochemical oxidation of Li_2S but also improves S utilization by generating a passive film on the Li metal negative electrode.[16] Cycling tests of Li_2S/KB@Cf electrodes were carried out under conditions of differnent S loadings and E/S ratios, as shown in **Figure 6**. The elctrochemical performance of electrodes with different S loadings at a current density of 0.3 mA cm^{-2} are shown in Figure 6(a,b). Cycling stability of cells vary slightly with the Li_2S loadings, capacities of 589, 660, 665 mAh g^{-1} of Li_2S were maintained after 50 cycles for electrodes with Li_2S loadings of 3.52, 7.21 and 10.08 mg cm^{-2}, respectively, indicating good stability of high S loading electrodes with Al foam. In this case, cell with lower loadings exhibited lower capacity rentention during cycling, which can be attributed to the dissolution of polysulfides into the electrlyte.[17] In the representative voltage profiles, after 50 cycles, flat plateaus in the range of 2.1-1.7V can still be observed with all Li_2S loadings. The 1.7-2.1 V plateau, which corresponds to the conversion from lower ordered ploysulfides to Li_2S, further indicates both

good electronic and ionic conductivity of the high loading electrodes with Li_2S/KB@Cf active material and Al foam.

In seeking a practical view of how the E/S ratio affects the cell performance of high loading elctrodes, a study of the cycling performance of electrodes with Li_2S loadings above 10 mg cm^{-2} at a current density of 0.3 mA cm^{-2} with differnt E/S ratios was carried out with the results shown in Figure 6(c). In an Al foam current collector, the 3-D structure is favorable for delivering electrons to the the entire volume of the Li_2S actie material. On the other hand, the pores within the electrode act as channels for electrolyte to facilitate Li ion transport, which further results in the improvement of electrode performance. It should be stated that good cycling stability can be obtained with E/S ratios below 10, as shown in Figure 6(c). When being cycled at a current density of 0.3 mA cm^{-2}, high capacities of 645 mAh g^{-1} (10.798 mg cm^{-2}) and 633 mAh g^{-1} (10.465 mg cm^{-2}) could be retaind for E/S ratios of 5.5 and 7 after 50 cycles, respectively. However, when the E/S fatio is reduced ratio to 4, the specific capacity underwent an abrupt drop after 10 cycles and kept decreasing, which can be atrributed to low ionic conductivity caused by less contact between the active material and the elctrolyte. The charge/discharge profiles of the 10th cycle of electrodes with different E/S ratios are shown in Figure 6(d). The c.ells with E/S ratios of 5.5 and 7 show stable and reversible plateaus. An increased overpotential in the discharge curve of the cell with an E/S ratio of 4 can be seen in Figure 6(d). This is probably because during the discharge process, the Li^+ concentration inside of the porous structure of the electrode continuesly decreases due to the consumption of Li^+. With a lower volume of elctrolyte and a higher active material loading, the Li^+ ions inside of the porous structure re consumed at an erlier stage of the discharge which can result in slower nucleation of Li_2S particles leading to low S utilization. To further highlight the importance of the Al foam in high S utilization and cycling stability, Li_2S/KB@Cf electrodes of relatively lower Li_2S loadings were cycled with Al foam and foil as currenet collector at a current density of 0.8 mA cm^{-2}, respectively, as shown in **Figure S6**.

As expected, after 40 cycles, cell with Al foam showed higher capacity and cycling stability while the capacity of the cell using Al foil as the current collector gradually decreased during prolonged cycling.

In order to facilitate Li_2S nucleation during discharge and compensate for the capacity loss caused by polysulfide dissolution with high Li_2S loading electrodes, a small amount of Li_2S_9 (0.08M) was used an electrolyte additive.[15b, 18] In this case, the specific capacity was calculated based on the total amount of active material in the cell including that in the eletrolyte. The long-term cyclability of Li_2S/KB@Cf electrode (11.29 Li_2S mg cm^{-2}, 75% Li_2S) was also demonstrated with a E/S ratio of 5.5 (Figure 6e). The cell showed excellent stability during cycling. After 100 cycles, the cell still delivered an areal capacity of 7.55 mAh cm^{-2} of Li_2S (10.8 mAh cm^{-2} of S) at 0.3 mA cm^{-2}. It is notable that a coulombic efficiency above 98% was maintained and a capacity retention of 80% was obtained after 100 cycles due to the presence of the additional polysulfides in the electrolyte. The voltage profiles at different cycles exhibited clear plateaus as in previous results (Figure 6f), which also indicated the high electronic and ionic conductivity of the electrode. **Figure S7** shows the cyclability of an electrode using as-prepared Li_2S/KB nanocomposite as active material.It was found that under the same test conditions, this cell shows lower S utilization and cycling stability, ans the voltage profiles exhibit high overpotential during discharging. It can be concluded that even though Al foam can provide a conductive framwork for facilitaed charge transfer, without the assistance of carbon fibers, the long-range electronic conductivity inside the electrode material is still insufficient and leads to a lower energy density.

The rate capability of cells with perpared Li_2S/KB and Li_2S/KB@Cf nonocomposite as active materials were investigated with an E/S ratio of 5.5 and Li_2S loadings both above 9 mg cm^{-2}. As shown in **Figure 7**(a), the Li_2S/KB@Cf electrode shows higher S utilization and better cycling stabiity, which can be attributed to the long-range electronic conductivity provided by the in-situ formed carbon fibers. The Li_2S/KB@Cf electrode shows a specific

capacity of 860 mAh g^{-1} to 431 mAh g^{-1} of Li_2S (1236 mAh $g^{-1}$to 620 mAh g^{-1} of S) at 0.1 mA cm^{-2} to 0.8 mA cm^{-2} (the 10th cycle at each current density) and typical charge/discgarge profiles were obtained at each current density, as displayed in Figure 7(b). Furthermore, the SEM image of cycled Li2S/KB@Cf electrode with a Li_2S loading of 10.6 mg cm^{-2} (Figure S6) shows that a crack-free electrode is well maintained during cycling, indicating mechanical stability of the high loading electrode with Al foam. In a more practical configuration, a pouch cell with a Li_2S/KB@Cf electrode (3x4 cm) and a lithium foil (500um thick) as counter electrode was assembled. Figure 7(c) illustrates the cycling performance of the pouch cell at 0.2 mA cm^{-2} with E/S ratio of 4.4. With a Li_2S loading of 10.2 mg cm^{-2}, a specific capacity of 637 mAh g^{-1} of Li_2S (915 mAh g^{-1} of S) was achieved after 48 cycles, demonstrating good conductivity and cycling stability. The relatively higher polarization of the discharge profiles shown in Figure 7(d) may be due to insufficient pressure during cell operation.

2.3. Characterization of high loading electrodes

To further investigate the electrochemical behavior of Li_2S/KB@Cf electrode with high Li_2S loading, cyclic voltammetry (CV) was carried out for 10 cycles at a scan rate of 0.15mV s^{-1}. The cell was charged to 4 V for the first cycle and followed by a sweeping between 1.7 V and 2.8 V, as displayed in **Figure S7**. Typical redox peaks associated with the stepwise reactions between Li_2S and S_8 can be observed as in previous work. The electrochemical reaction kinetics of Li_2S/KB@Cf electrode with high Li_2S loading was also examined at different charge/discharge stages by electrochemical impedance spectroscopy, as shown in **Figure S8**. The cell with a Li_2S loading of 11.2 mg cm^{-2} exhibits low Ohmic resistance at high frequencies and a semicircle corresponding to the charge transfer resistance can be defined in the medium to high frequency range,[10c] suggesting high electronic conductivity and fast electrochemical kinetics. Relatively high mass transport rates can also be conclued from the low frequency range for the high loading electrode due to the porous structure of the electrode, providing for fast ion transfer.

For the purpose of understanding the electrochemical charge/discharge behavior of the Li_2S/KB@Cf electrode under real operation conditions, we also performed in situ and operando X-ray absorption spectroscopy (XAS) experiments. For the XAS tests, the electrode sluury was coated onto Al foam and 1 M LiClO4 in dioxolane (DOL)/dimethoxyethane (DME) (1:1, by volume) was used as the electrolyte. The advantge of XAS is that it is element-specific and can be used to detect species that are amorphous or crystalline. **Figure 8**(a-c) show the sulfur K-edge XAS maps (XAS intensity as a function of photon energy and specific capacity) accompanied with the corresponding voltage profiles for the first charge, first discharge, and second charge processes, respectively. For comparison, the spectra of elemental sulfur, lithium polysulfides, as-synthesized Li_2S/KB@Cf material and Li_2S/KB@Cf in the coin cell are also shown in Figure 8d. For Li_2S in the coin cell, the initial spectrum shows two features at about 2473.2 and 2475.7 eV, which is in good agreement with previous results. The features at about 2476.2 and 2478.8 eV originate from the surface oxidization of Li_2S induced by the electrolyte. During the first charge process (Figure 8a), the feature at 2473.2 eV continuously increases, indicating the conversion from Li_2S to sulfur. During the whole first charge, no signature of polysulfides at 2470.5 eV is observed, which implies that Li_2S is directly converted to sulfur without the formation of polysulfides. The XAS results are in good agreement with what we proposed previously [add reference here}.

During the first discharge process (Figure 8b), the feature of sulfur is continuously decreasing with a gradual increase of the polysulfide signature. This observation indicates the sulfur is transformed first to polysulfides and then to Li_2S. However, the feature of polysulfides is still clearly observed at the end of first discharge, indicating that not all polysulfides are converted to Li_2S. In contrast, the XAS spectra of the second charge (Figure 8c) also shows a gradual increase of the feature at ~2473 eV resulting from the transformation from Li_2S to sulfur, while the feature of polysulfides is still visible. We propose that Li_2S is first oxidized to

polysulfides and then to sulfur during the second charge. The different charging mechanism for the first and second cycles originates from the residual polysulfides at the end of the first discharge, which can not only reduce the charge-transfer resistance at the Li_2S/electrolyte interface but also facilitate the transformation from Li_2S to polysulfides.

3. Conclusion

Targeting for the application of the Li/S cell with superior specific energy and long cycle life, a Li_2S/KB@Cf composite as active material was developed through a facile yet productive strategy. A uniform distribution of KB particles and conformal carbon coating after RCVD not only helps suppress the polysulfide dissolution but also effectively facilitates the fast transport of electrons. More importantly, high long-range electronic conductivity achieved through the in-situ formed carbon fibers formed via RCVD can also guarantee fast reaction kinetics, reduced polarization and improved cyclability of the cell. To fulfill the requirement for high S loading, a 3-D interconnected Al foam was applied as current collector which provided the capability to increase the active material loading while maintaining high structural stability. Furthermore, the conductive porous architecture of Al foam can facilitate fast charge and ion transfer to all of the active material, which brings improvements in cycling stability and utilization of active material. The electrolyte/S (E/S) ratio, one of the critical parameters for a high-specific energy system, was significantly reduced in this work. As a result, a high areal capacity of 7.55 mAh cm^{-2} and high coulombic efficiency were retained after 100 cycles with an E/S ratio of 5.5. Although excellent performance was obtained with high Li_2S loading (> 10 mg cm^{-2}) and low E/S ratio (<5) in this paper, however, electrolyte depletion was also ovserved after cycling which is mainly due to the decomposition and reaction of electrolyte solvents toward lithium metal and reaction intermediates. The specific power of Li/S cells also needs more investigation to be qualified for some practical applications. Therefore, for future research associated with the Li/S system, the opportunities and challenges are still calling for intensive study and improved technologies.

4. Experimental Section

Active Material Synthesis: Commercial Li_2SO_4 particles were re-precipitated using an anti-solvent method to obtain uniformly fine particles. Li_2SO_4 was firstly dissolved in 20 mL deionized water till saturation, then a certain amount of reagent ethanol (anhydrous, ≥99.5%) was added into Li_2SO_4 solution dropwise, allowing Li_2SO_4 particles to precipitate. Separated layers were formed in the mixture after all the Li_2SO_4 was re-precipitated. The milky suspension was filtered and washed with ethanol. The as-prepared $Li_2SO_4 \cdot H_2O$ powder was then vacuum dried at 140 ˚C overnight to remove the remaining ethanol and the water of crystallization.

The Li_2S/KB composite was synthesized based on the following chemical reaction: $Li_2SO_4 + C \rightarrow Li_2S + CO_2\uparrow$. 1.2g Li_2SO_4 was dispersed in 150 mL ethanol containing 400mg polyvinylpyrrolidone (PVP; Mw~1,300K) under ultra-sonication for 1h. Then different amounts (330~420mg) of ketjen black (KB, EC-600JD) were added into the prepared solution and stirred at room temperature overnight. Finally, the mixture was filtered and washed with ethanol several times to remove excess PVP. After being dried at 50 ˚C in a vacuum oven overnight, the as-synthesized PVP-modified Li_2SO_4/KB was heat-treated in a tube furnace at 820 ˚C for 30min under flowing argon gas with a controlled flow rate of 100cc/s. Li_2S/KB composites without PVP modification were also prepared using the same procedure for comparison. To precisely estimate the weight ratio of Li_2S in the Li_2S/KB composite, a certain amount of Li_2S/KB was weighted and washed with deionized water via filtration for several times until the pH of the filtered solution reached 7, comparing the weight difference between powder before and after being washed with deionized water provides the weight percentage of Li_2S (75 wt.%-85 wt.%).

The Li_2S/KB@Cf composite was prepared using a facile Rotating Chemical Vapor Deposition (RCVD) method to ensure uniform fiber growth. The Li_2S/KB composite was heated to 700℃ for 30min in a lab-designed rotating furnace using argon gas and acetylene

(carbon precursor) with a flow rate of 100 SCCM (standard cubic centimeters per minute) and 10SCCM, respectively. The amount of carbon fibers formed can be calculated by weighting the composite before and after the RCVD procedure (~5 wt.%).

Materials Characterization: Due to the high sensitivity of Li_2S towards moisture, preparation of all the samples for characterization was conducted in an argon-filled glove box with a moisture content below 0.1 ppm and oxygen content below 0.6 ppm. Investigations of the crystal structure of samples were conducted using an X-ray diffractometer (XRD, Bruker AXS D8 Discover GADDS microdiffractometer) with a Co Kα radiation source. Samples were protected from moisture using an air-free holder. The morphology of synthesized active material and electrodes was observed using a field emission scanning electron microscope (FESEM, JEOL JSM-7500F) with elemental mapping using energy-dispersive X-ray spectroscopy (EDS, Oxford). The in-situ and operando sulfur K-edge XAS spectra were investigated using a bend magnet beam line with photon energy ranging from 1000 to 13,000 eV at beamline 5.3.1 (Advanced Light Source, Lawrence Berkeley National Laboratory). All the in-situ XAS tests were conducted under constant helium flow in the sample chamber during cell cycling. The XAS spectra were studied in total fluorescence yield mode and calibrated using elemental sulfur spectra by setting the white line position to 2472.2 eV.

Electrochemical Measurements : For electrode slurry preparation, Li_2S, carbon materials (including KB, carbon fibers obtained from RCVD and carbon black as conducting agent) and binders (SBR: PVP, 1:1 in weight) were mixed together with different weight ratios. Li_2S electrodes were fabricated by coating the slurry on aluminum foil or drop-casting on aluminum foam, respectively. Electrolyte was prepared by dissolving 1.2M LiTFSI (Lithium Bis(Trifluoromethanesulfonyl)Imide) in DOL(dioxolane)/DME(Dimethoxyethane) (1:1, by volume) containing 0.3M $LiNO_3$ (lithium nitrate). For cells with higher S loadings, 0.08M Li_2S_9 and 0.5M LiTFSI in DOL/DME (1:1, by volume) containing 0.1M $LiNO_3$ was used as electrolyte.

CR2325 coin cells were assembled in an argon filled glove box. The cell consisted of the electrodes fabricated, lithium metal foil ngative electrode (99.98%, Cyprus Foote Mineral) and a porous polypropylene separator (2400, Celgard). Electrochemical performance of the cells was evaluated with a battery cycler (Maccor S4000) between 1.7-2.7/2.8V after being charged to 4V for the first charge in order to activate the Li_2S. Cyclic voltammetry (CV) and Electrochemical Impedance Spectroscopy (EIS) tests of the coin cells were conducted using an electrochemistry tester (EC-Lab VMP3) in the range 1.7- 2.8V after being firstly charged to 4.0V.

Supporting Information

Supporting Information is available from the Wiley Online Library.

Acknowledgements

Work in the Energy Technologies Area of Lawrence Berkeley National Laboratory was supported by CERDEC U.S. ARMY under project No.104302. We thank Tevye Kuykendall and the Molecular Foundry of the Lawrence Berkeley National Laboratory for supporting the X-ray diffractometer and scanning electron microscope. Work at the Molecular Foundry was supported by the Office of Science, Office of Basic Energy Sciences, of the U.S. Department of Energy under Contract No. DE-AC02-05CH11231. The work at Advanced Light Source of the Lawrence Berkeley National Laboratory was supported by the Director, Office of Science, Office of Basic Energy Sciences, of the U.S. Department of Energy under Contract No. DE-AC02-05CH11231.

References

[1] a) M. S. Whittingham, *Science*, **1976**, 192, 1126; b) M. Winter,R. J. Brodd, *Chem Rev*, **2004**, 104, 4245.

[2] a) J. M. Tarascon,M. Armand, *Nature*, **2001**, 414, 359; b) B. Dunn, H. Kamath,J. M. Tarascon, *Science*, **2011**, 334, 928; c) Z. Yang, J. Zhang, M. C. Kintner-Meyer, X. Lu, D. Choi, J. P. Lemmon,J. Liu, *Chem Rev*, **2011**, 111, 3577; d) J. B. Goodenough, *Acc Chem Res*, **2013**, 46, 1053; e) J. B. Goodenough,K. S. Park, *J Am Chem Soc*, **2013**, 135, 1167.

[3] a) P. G. Bruce, S. A. Freunberger, L. J. Hardwick,J. M. Tarascon, *Nat Mater*, **2012**, 11, 19; b) A. Manthiram, Y. Z. Fu,Y. S. Su, *Accounts Chem Res*, **2013**, 46, 1125; c) S.-E. Cheon, K.-S. Ko, J.-H. Cho, S.-W. Kim, E.-Y. Chin,H.-T. Kim, *J Electrochem Soc*, **2003**, 150, A796; d) M. K. Song, E. J. Cairns, Y. Zhang, *Nanoscale*, **2013**, 5, 2186; e) A. Manthiram, S. H. Chung,C. X. Zu, *Adv Mater*, **2015**, 27, 1980; f) M. Hagen, D. Hanselmann, K. Ahlbrecht, R. Maca, D. Gerber,J. Tubke, *Adv Energy Mater*, **2015**, 5, ; g) S. Urbonaite, T. Poux,P. Novak, *Adv Energy Mater*, **2015**, 5, 1500118.

[4] a) K. Cai, M. K. Song, E. J. Cairns, Y. Zhang, *Nano Lett*, **2012**, 12, 6474; b) C. X. Zu, M. Klein,A. Manthiram, *J Phys Chem Lett*, **2014**, 5, 3986; c) Y. Yang, M. T. McDowell, A. Jackson, J. J. Cha, S. S. Hong,Y. Cui, *Nano Lett*, **2010**, 10, 1486.

[5] a) Y. C. Qiu, G. L. Rong, J. Yang, G. Z. Li, S. Ma, X. L. Wang, Z. H. Pan, Y. Hou, M. N. Liu, F. M. Ye, W. F. Li, Z. W. Seh, X. Y. Tao, H. B. Yao, N. Liu, R. F. Zhang, G. M. Zhou, J. P. Wang, S. S. Fan, Y. Cui,Y. G. Zhang, *Adv Energy Mater*, **2015**, 5, ; b) Y. Chen, S. T. Lu, J. Zhou, W. Qin,X. H. Wu, *Adv Funct Mater*, **2017**, 27, ; c) G. Liu, S. Xun, N. Vukmirovic, X. Song, P. Olalde-Velasco, H. Zheng, V. S. Battaglia, L. Wang,W. Yang, *Adv Mater*, **2011**, 23, 4679; d) H. B. Lin, L. Q. Yang, X. Jiang, G. C. Li, T. R. Zhang, Q. F. Yao, G. W. Zheng,J. Y. Lee, *Energ Environ Sci*, **2017**, 10, 1476; e) S. Evers,L. F. Nazar, *Accounts Chem Res*, **2013**, 46, 1135.

[6] a) X. Ji, K. T. Lee,L. F. Nazar, *Nat Mater*, **2009**, 8, 500; b) J. Nelson, S. Misra, Y. Yang, A. Jackson, Y. Liu, H. Wang, H. Dai, J. C. Andrews, Y. Cui,M. F. Toney, *J Am Chem Soc*, **2012**, 134, 6337; c) C. Nan, Z. Lin, H. Liao, M. K. Song, Y. Li, E. J. Cairns, *J Am Chem Soc*, **2014**, 136, 4659; d) Z. W. Seh, H. T. Wang, P. C. Hsu, Q. F. Zhang, W. Y. Li, G. Y. Zheng, H. B. Yao,Y. Cui, *Energ Environ Sci*, **2014**, 7, 672; e) S. Walus, C. Barchasz, R. Bouchet, J. C. Lepretre, J. F. Colin, J. F. Martin, E. Elkaim, C. Baehtz,F. Alloin, *Adv Energy Mater*, **2015**, 5, ; f) D. Sun, Y. Hwa, Y. Shen, Y. Huang, E. J. Cairns, *Nano Energy*, **2016**, 26, 524; g) L. Zhang, D. Sun, J. Feng, E. J. Cairns, J. H. Guo, *Nano Lett*, **2017**, 17, 5084; h) F. Y. Fan, W. C. Carter,Y. M. Chiang, *Adv Mater*, **2015**, 27, 5203.

[7] a) D. P. Lv, J. M. Zheng, Q. Y. Li, X. Xie, S. Ferrara, Z. M. Nie, L. B. Mehdi, N. D. Browning, J. G. Zhang, G. L. Graff, J. Liu,J. Xiao, *Adv Energy Mater*, **2015**, 5, ; b) H.-J. Peng, J.-Q. Huang, X.-B. Cheng,Q. Zhang, *Adv Energy Mater*, **2017**, 1700260.

[8] Z. Wang, Y. Dong, H. Li, Z. Zhao, H. B. Wu, C. Hao, S. Liu, J. Qiu,X. W. Lou, *Nat Commun*, **2014**, 5, 5002.

[9] M. Hagen, P. Fanz,J. Tubke, *J Power Sources*, **2014**, 264, 30.

[10] a) S. Zhang, M. N. Liu, F. Ma, F. M. Ye, H. F. Li, X. Y. Zhang, Y. Hou, Y. C. Qiu, W. F. Li, J. Wang, J. Wang,Y. G. Zhang, *J Mater Chem A*, **2015**, 3, 18913; b) D. H. Wang, X. H. Xia, D. Xie, X. Q. Niu, X. Ge, C. D. Gu, X. L. Wang,J. P. Tu, *J Power Sources*, **2015**, 299, 293; c) J. Zhang, Y. Shi, Y. Ding, L. L. Peng, W. K. Zhang,G. H. Yu, *Adv Energy Mater*, **2017**, 7, 1602876.

[11] F. X. Wu, H. Kim, A. Magasinski, J. T. Lee, H. T. Lin,G. Yushin, *Adv Energy Mater*, **2014**, 4, 1300655.

[12] a) G. He, S. Evers, X. Liang, M. Cuisinier, A. Garsuch,L. F. Nazar, *Acs Nano*, **2013**, 7, 10920; b) J. Schuster, G. He, B. Mandlmeier, T. Yim, K. T. Lee, T. Bein,L. F. Nazar, *Angew Chem Int Ed Engl*, **2012**, 51, 3591; c) C. F. Zhang, H. B. Wu, C. Z. Yuan, Z. P. Guo,X. W.

Lou, *Angew Chem Int Edit*, **2012**, 51, 9592; d) M. K. Song, Y. G. Zhang, E. J. Cairns, *Nano Lett*, **2013**, 13, 5891.

[13] M. A. Lowe, J. Gao,H. D. Abruna, *Rsc Adv*, **2014**, 4, 18347.

[14] a) Y. Fu, C. Zu,A. Manthiram, *J Am Chem Soc*, **2013**, 135, 18044; b) Q. Sun, X. Fang, W. Weng, J. Deng, P. N. Chen, J. Ren, G. Z. Guan, M. Wang,H. S. Peng, *Angew Chem Int Edit*, **2015**, 54, 10539; c) F. Y. Jin, S. Xiao, L. J. Lu,Y. Wang, *Nano Lett*, **2016**, 16, 440.

[15] a) M. Yu, J. Ma, M. Xie, H. Song, F. Tian, S. Xu, Y. Zhou, B. Li, D. Wu, H. Qiu,R. Wang, *Adv Energy Mater*, **2017**, 1602347; b) L. Qie, C. X. Zu,A. Manthiram, *Adv Energy Mater*, **2016**, 6, 1502459.

[16] A. Jozwiuk, B. B. Berkes, T. Weiß, H. Sommer, J. Janek,T. Brezesinski, *Energy Environ. Sci.*, **2016**, 9, 2603.

[17] a) Y. V. Mikhaylik,J. R. Akridge, *J Electrochem Soc*, **2004**, 151, A1969; b) J. Conder, R. Bouchet, S. Trabesinger, C. Marino, L. Gubler,C. Villevieille, *Nat Energy*, **2017**, 2, 17069 ; c) Y. Diao, K. Xie, S. Z. Xiong,X. B. Hong, *J Electrochem Soc*, **2012**, 159, A421.

[18] a) D. J. Lee, M. Agostini, J. W. Park, Y. K. Sun, J. Hassoun,B. Scrosati, *Chemsuschem*, **2013**, 6, 2245; b) X. W. Yu,A. Manthiram, *Phys Chem Chem Phys*, **2015**, 17, 2127.

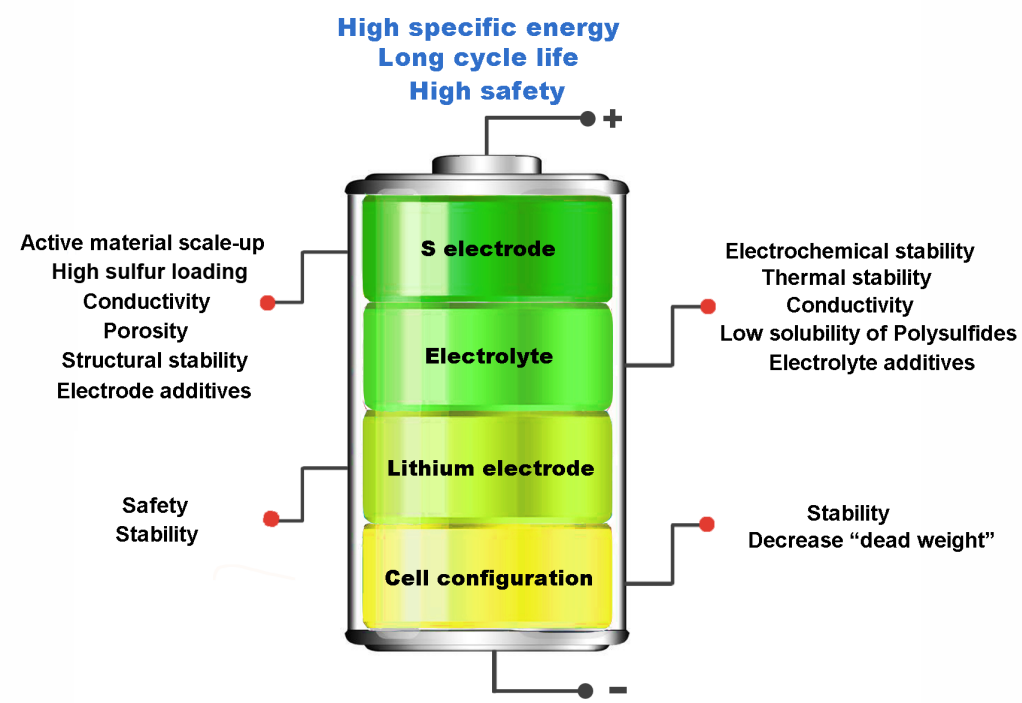

Figure 1. Illustrated scheme of modifications of each cell component.

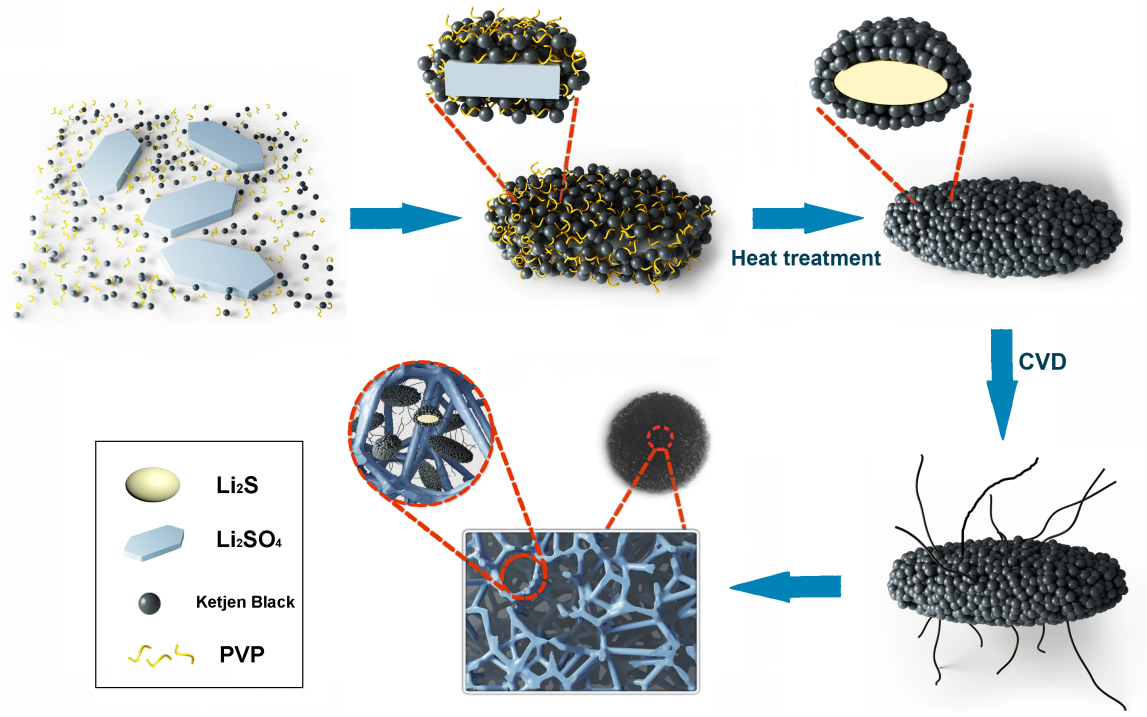

Figure 2. Schematic illustration of Li_2S/KB@Cf nano-composite and Li_2S electrode.

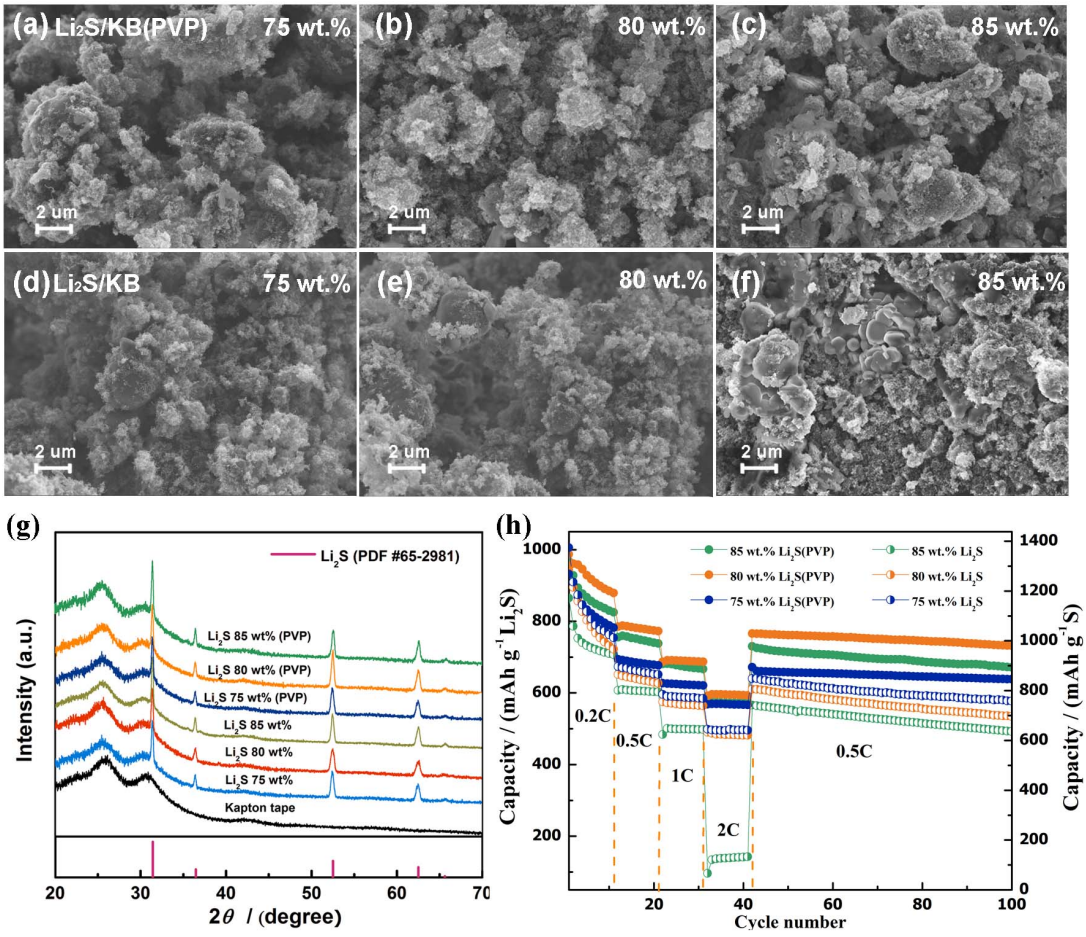

Figure 3. (a-f) SEM images of Li_2S/KB composites of different Li_2S weight fractions with and without adding PVP during synthesis process. (g) X-ray diffraction patterns of the synthesized Li_2S/KB composites. Cobalt was used as XRD source. (h) Rate performance of the Li_2S/KB cathodes at different discharge C rates from 0.2 C to 2.0 C. Li_2S loading: ~1.5 mg cm^{-2}.

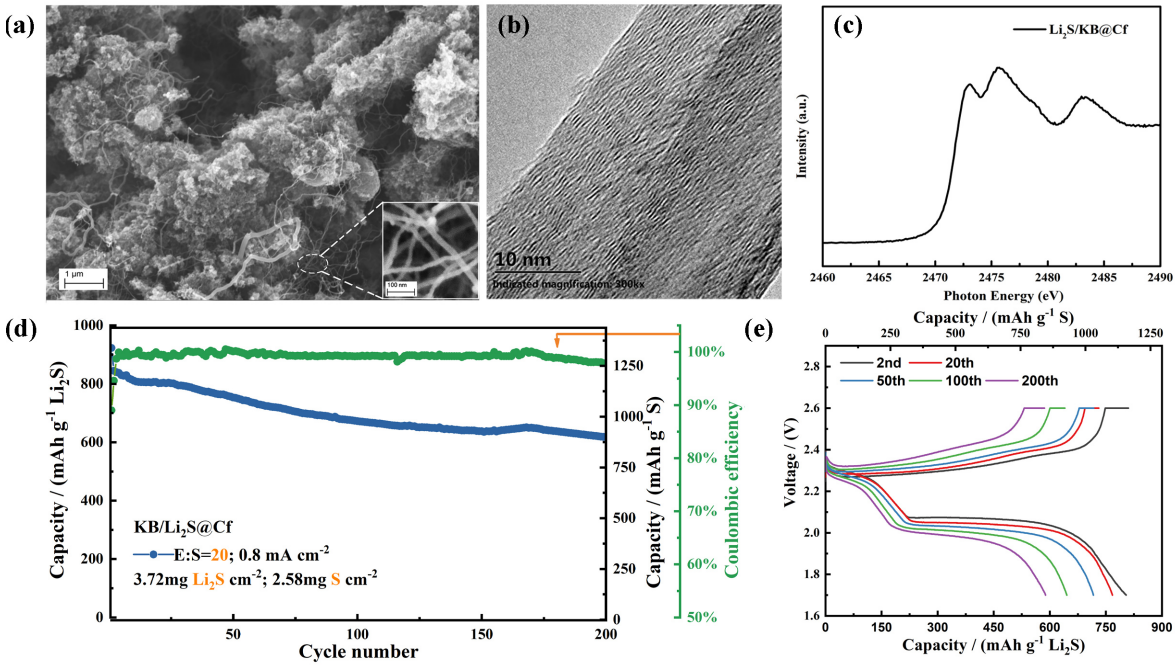

Figure 4. (a) SEM images of as synthesized Li_2S/KB@Cf composite; (b) TEM result of carbon fiber produced via RCVD process; (c) XAS spectrum of as prepared Li_2S/KB@Cf material; (d) Cycling performance of the Li_2S/KB@Cf electrode at a current density of 0.8 mA cm^{-2} with Al foil as current collector. (e) Corresponding charge and discharge voltage profiles of the Li_2S/KB@Cf electrode

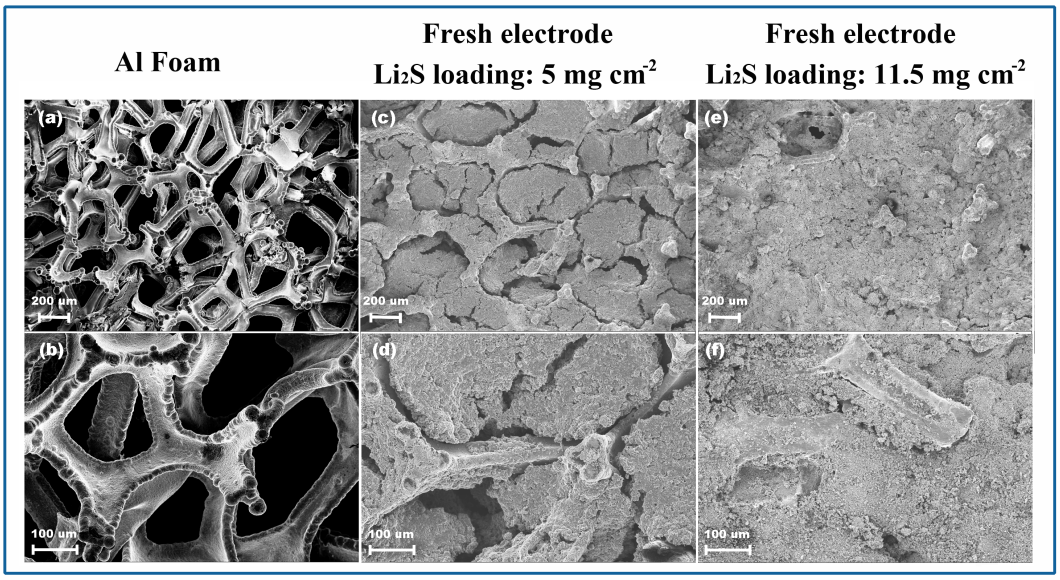

Figure 5. SEM images of (a, b) pristine Al foam; (c-f) fresh Li_2S/KB@Cf electrodes with different Li_2S loadings.

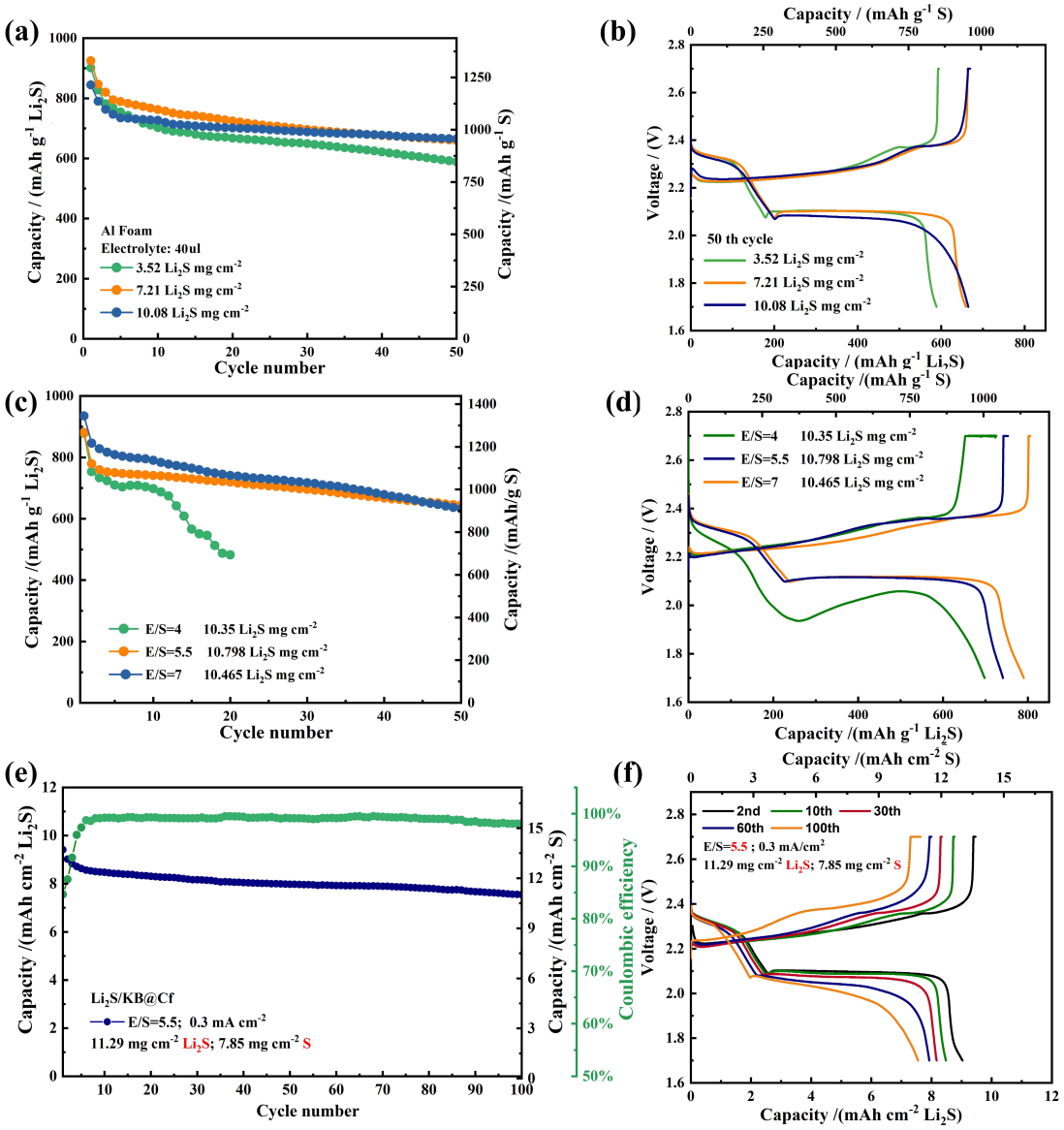

Figure 6. Cycling properties and representative charge/discharge profiles of Li_2S/KB@Cf electrodes with (a, b) different Li_2S loadings; (c, d) different E/S ratios and (e, f) optimized configuration. Current density: 0.3 mA cm^{-2}.

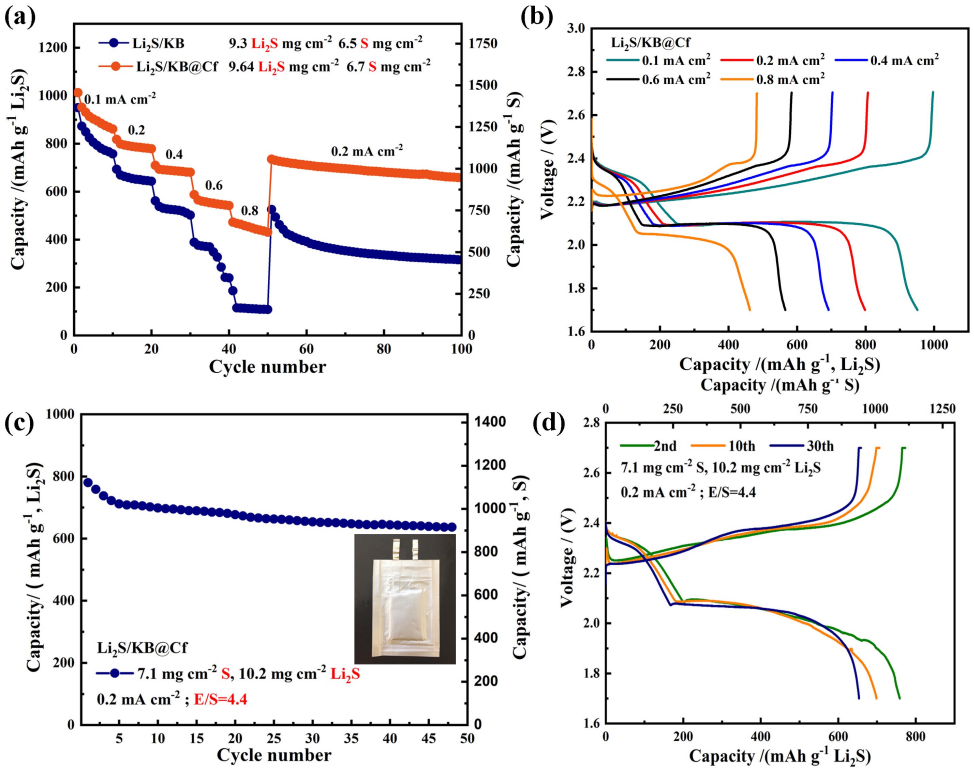

Figure 7. (a, b) Comparsion of Rate capability between high loading Li_2S electrode with and without insitu-formed carbon fibers. (c,d) Cycling performance and discharge/charge curves of a high Li_2S loading Li/Li_2S pouch cell (2 electrode cell, 3X4 cm) with the low E/S ratio of 4.4. Electrolyte composition: 0.5M LiTFSI in DOL/DME(1:1, v:v).

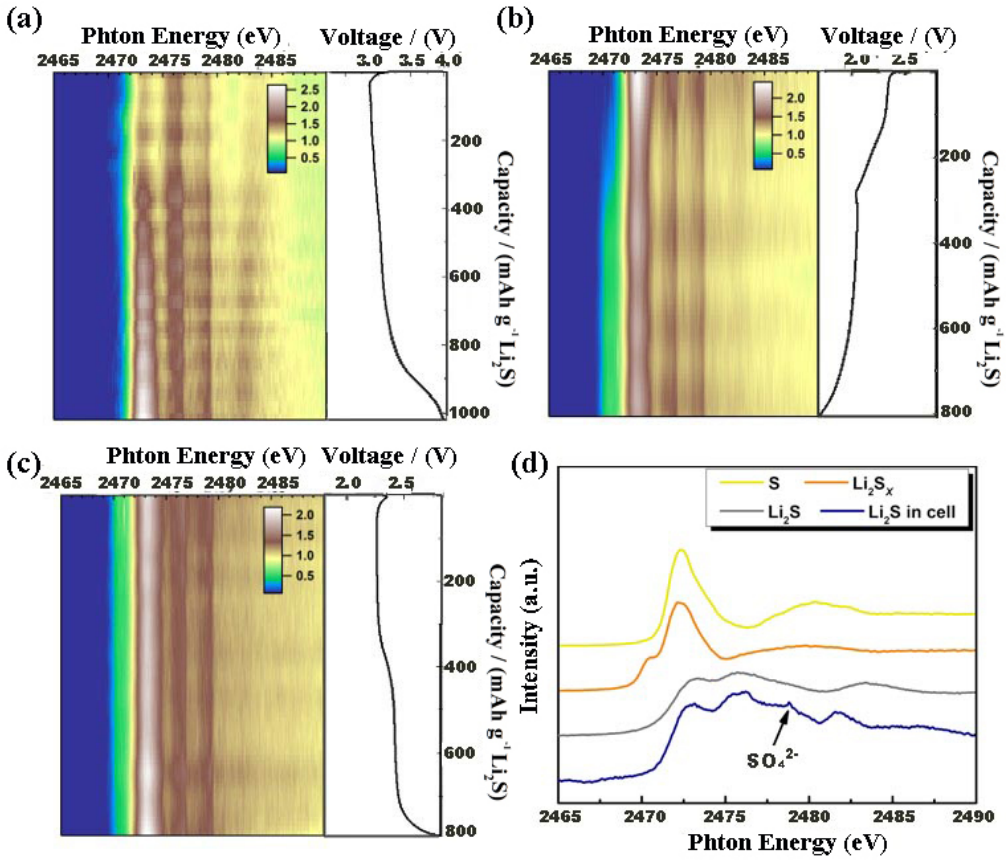

Figure 8. (a-c) *In situ and operando* sulfur K-edge XAS mapping and the corresponding voltage profile for the first charge, discharge and the second charge, respectively. (d) XAS spectrum of sulfur, PSs, as-synthesized Li_2S active material, and XAS spectrum of the Li_2S electrode in the cell.

Several investigations in cell configuration have been conducted to successfully obtain a Li/S cell with high active material loading and low E/S ratio while maintaining good performance. This work offers an exciting opportunity to develop the "beyond Li Ion" cell with specific energy greater than that of any rechargeable cell available today, at a lower cost, and with greater safety.

lithium/sulfur cell, lithium sulfide, high loading, electrolyte/sulfur ratio, aluminum foam

Dan Sun and Elton J. Cairns*

High lithium sulfide loading electrodes for practical Li/S cells with high specific energy

ToC figure

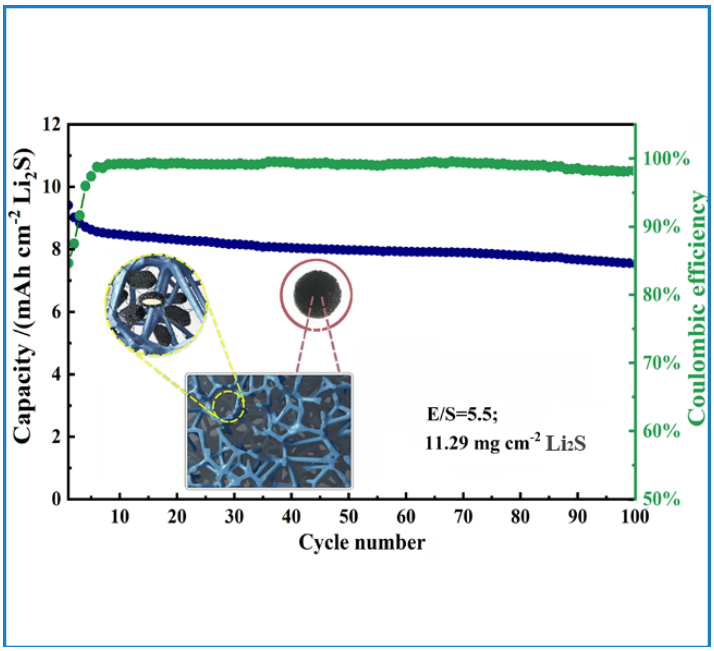

Supporting Information

High lithium sulfide loading electrodes for practical Li/S cells with high specific energy

Dan Sun, Yoon Hwa, Liang Zhang, Jingwei Xiang, Jinghua Guo, Yunhui Huang and Elton J. Cairns*

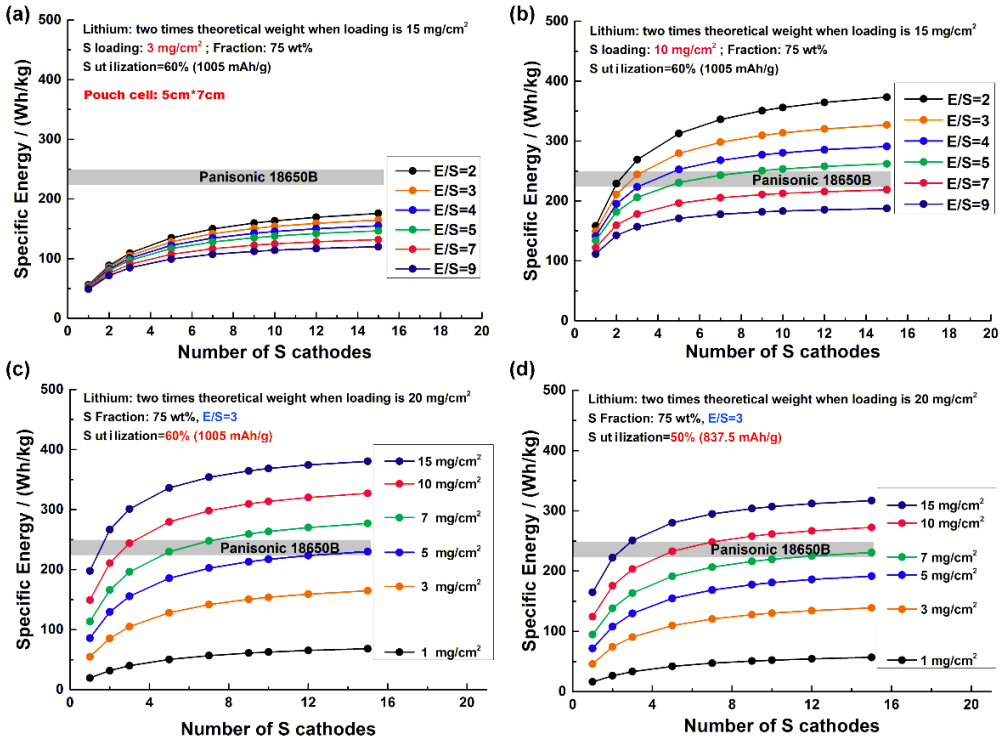

Figure S1 Calculated specific energy with different pouch cell configurations. (Electrode size: 5cm*7cm, all cell housings included.)

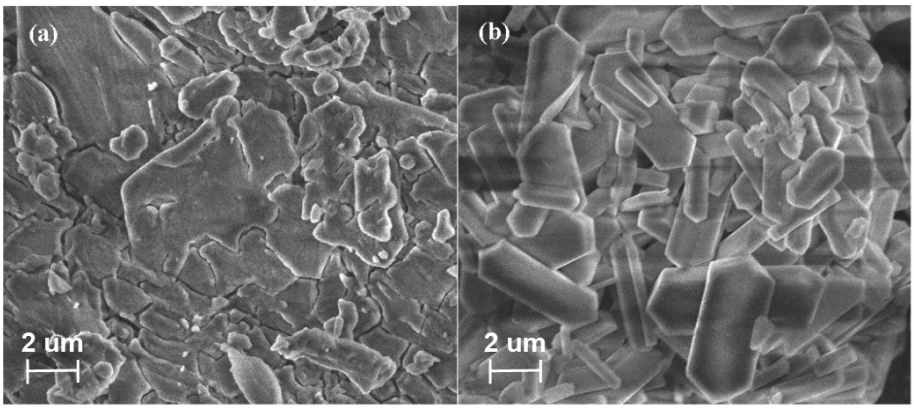

Figure S2. SEM images of commercial (a) and re-precipitated (b) Li_2SO_4.

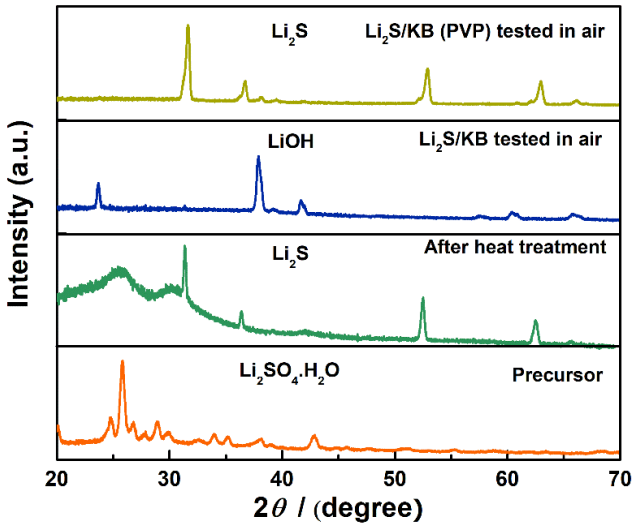

Figure S3. XRD patterns of precursor and different Li_2S/KB samples tested under different conditions. With the assistance of PVP during preparation, more conformal carbon protection was assured.

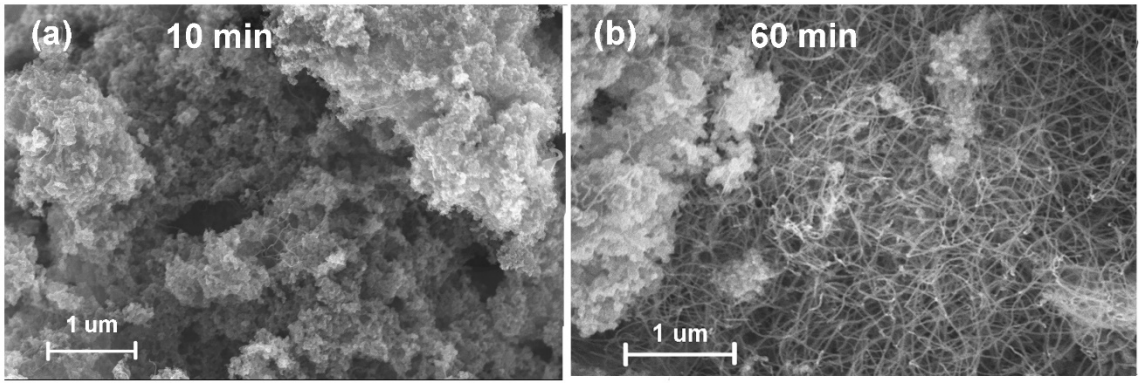

Figure S4. The influence of RCVD time on the amount of CNFs produced. (a) RCVD time is 10 minutes; (b)RCVD time is 60 minutes.

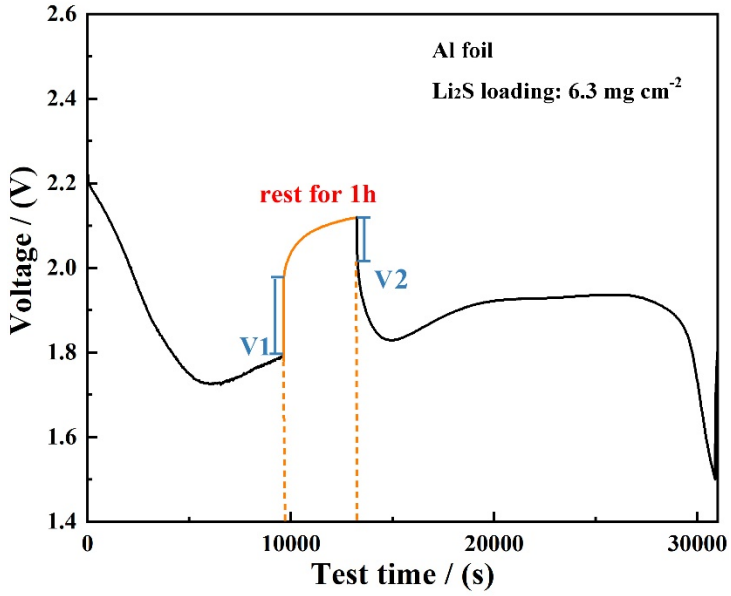

Figure S5. IR drop test of high S loading electrode with Al foil. V1 and V2 represent the voltage changes caused by both electron transfer and ion diffusion. During the rest time, if there's only a charge transfer problem, the voltage will remain the same since the voltage gap caused by impedances between interfaces inside of the cell do not change. If ion transfer problem existed, the voltage will gradually increase until the Li^+ concentration inside the porous structure and in the main electrolyte reaches the same, and the voltage change after rest would decrease.

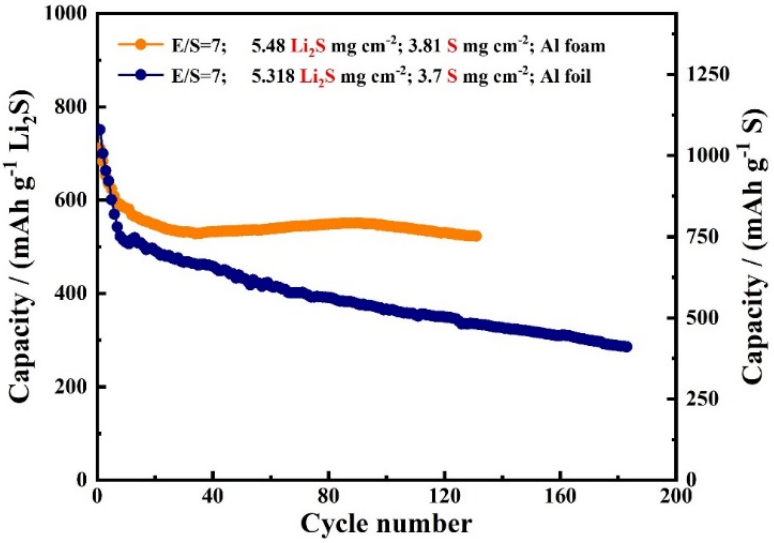

Figure S6. cycling performances of the Li_2S/KB@Cf electrodes using Al foam and foil as current collector with the E/S ratio of 5. Current density: 0.3 mA cm^{-2}.

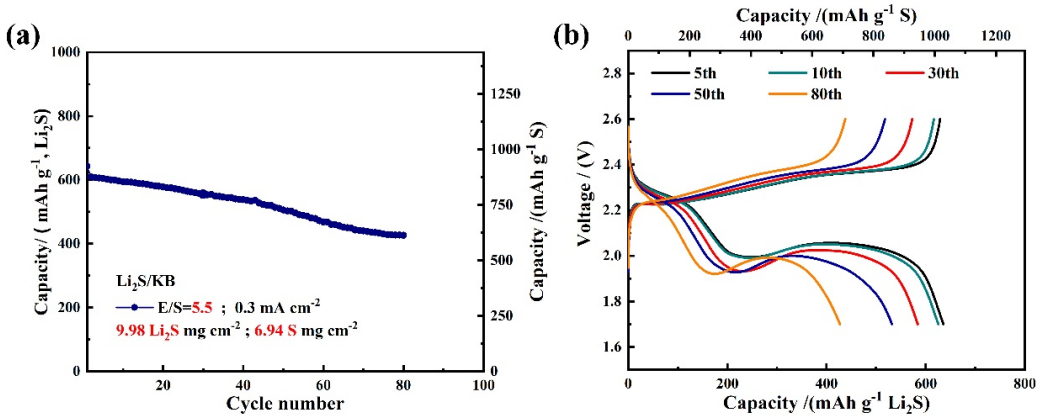

Figure S5. (a) Cycling performance and (b) discharge/charge profiles of high Li_2S loading electrodes without carbon fibers.

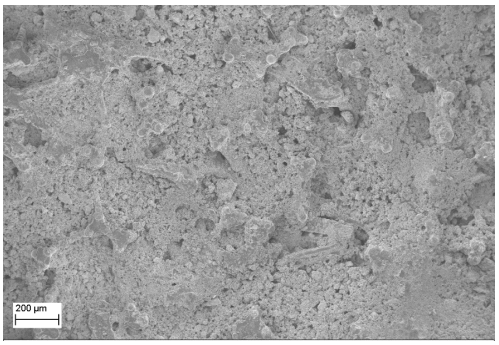

Figure S6. Cycled Li_2S/KB@Cf electrode after 45 cycles with a Li_2S loading of 10.6 mg cm^{-2}. Current density: 0.3 mA cm^{-2}.

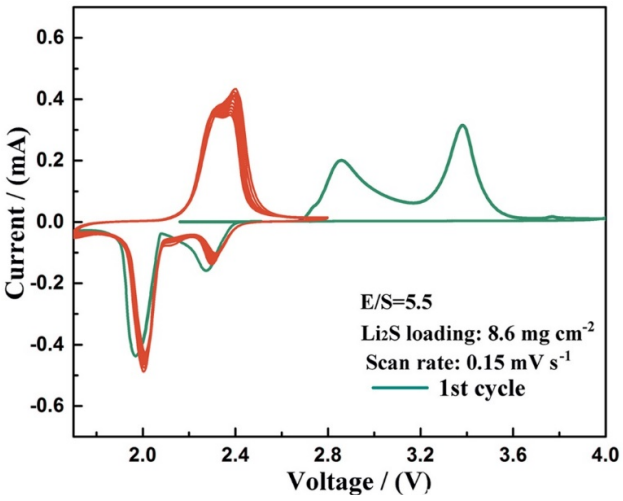

Figure S7. Cyclic voltammetry results of cells with Li_2S-KB@Cf as positive electrode active material.

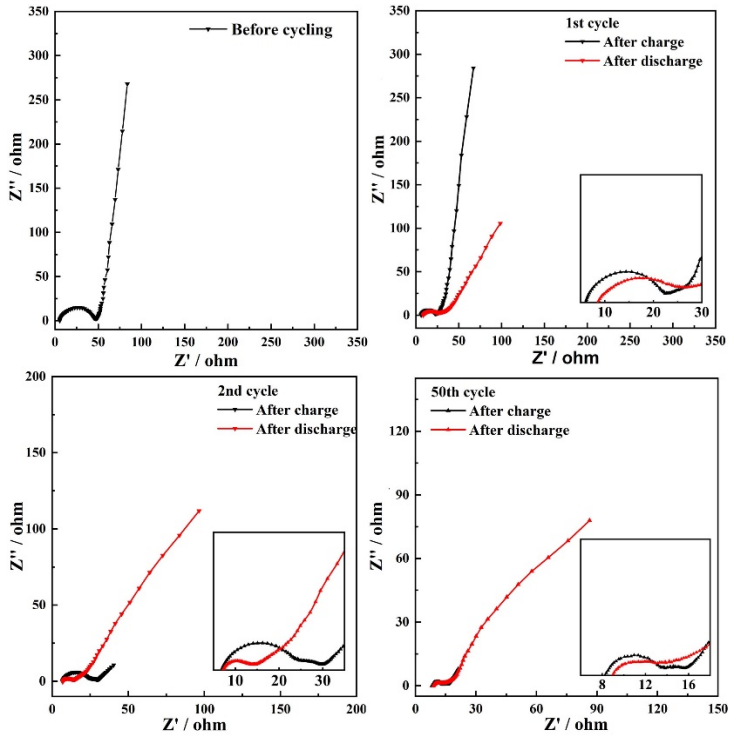

Figure S8. Electrochemical impedance spectroscopy results of the Li_2S/KB@Cf electrode. (Li_2S loading: 11.2 mg cm^{-2} ,75 wt.% Li_2S). E/S ratio=4.4. Electrochemical impedance was measured from 10 mHz to 1 MHz.